

Breast Imaging in Coronal Planes with Simultaneous Pulse Echo and Transmission Ultrasound

Abstract. *Clear delineation of breast architecture was achieved with compound pulse echo ultrasound imaging in which the images were acquired in the coronal planes used for quantitative transmission ultrasonic computed tomography. Since most connective tissue planes in the breast radiate toward the nipple, compound scans from the sides of the breast record normal interfaces more consistently and reveal greater symmetries in normal portions of relatively full breasts than do conventional scans in sagittal or transverse planes. Simultaneous acquisition of the pulse echo images and images representing the local ultrasound attenuation coefficient and speed of ultrasound suggested complementary roles for reflection and through-transmission images in breast cancer detection. The high quality of pulse echo images in coronal planes provides the potential for more complete pulse echo diagnosis and the basis for spatial correlation of lesions viewed in pulse echo and ultrasonic computed tomograms. These observations may permit routine ultrasonic computed tomography of the breast in the clinical setting.*

Ultrasonic computed tomography (UCT) refers to through-transmission ultrasound imaging performed and reconstructed in a manner similar to that employed in commercial x-ray computed tomography scanners. Since the first report on UCT in 1975 (1), numerous groups have attempted to improve the resolution and accuracy of these quantitative images and to increase the variety of the properties measured (2). Several studies of UCT in breast cancer detection have been performed or are in progress with small numbers of patients (3, 4). While some investigators expect the UCT images to be sufficient for breast cancer diagnosis, we believe that UCT must be combined with pulse echo ultrasound imaging because of the unique information that each technique provides on tissue structure and because of the relatively wide experience with pulse echo imaging.

The prevailing opinion that pulse echo images of the breast should be performed in planes other than the coronal planes required for UCT has impeded utilization of UCT for breast cancer diagnosis. In many earlier examinations of patients, our coronal UCT results complemented substantially the information from pulse echo images in transverse planes (4). However, it was not clear whether this information justified the development and routine use of separate UCT and pulse echo scanners or a more complex single system that could scan in coronal as well as transverse or sagittal planes. In a complex and nonrigid organ like the breast it was particularly difficult to be certain of spatial correlations between structures viewed in the two orthogonal sets of planes imaged by UCT and pulse echo modes.

These concerns have been greatly relieved in the past year, during which compound pulse echo images were ob-

tained simultaneously with the UCT attenuation and speed of sound information and in the same coronal planes. The ease and utility of spatial correlation between suspected masses in the UCT and pulse echo images are very promising. More important, exceptional clarity is provided by the coronal pulse echo images in most patients because of the unique anatomic symmetries in coronal planes and the normal orientation of these planes relative to most echogenic breast structures.

In the UCT pulse echo system the patient lies prone with one breast admitted into the scanning tank through a circular aperture in the table. The scanning tank is filled with degassed water at 20°C, for the best possible match of the speed of sound in water and fat. Submerged in the tank are the transducers used for UCT and pulse echo data acquisition (4). The transducers are mounted on opposing platforms on parallel slide

rails. Translation of the transducer platform and tank rotation are performed by stepper motors under computer control for translate-rotate CT geometry. Images of sequential coronal planes may be acquired by adjusting the height of the scanning tank. The transducers used for simultaneous pulse echo and CT transmission as well as pulse echo reception are 19 mm in diameter, long-focused, and have a center frequency of 3.5 MHz and 40 percent fractional bandwidth.

Salient features of the pulse echo system electronics include preamplification of the returning echoes prior to logarithmic amplification. At present, computer noise generated during computer-controlled scanning limits the system to a 55-dB dynamic range. Time gain compensation is triggered by the skin echo and is terminated midway through the breast, so each point is viewed from the 180° sector in which the point is nearest to the skin. The compound pulse echo image is generated on an analog scan converter that is now writing in the maximum amplitude mode; it is anticipated that a change to the integration mode will improve image quality. The UCT data are acquired every 2° over 180° and the pulse echo data are acquired for linear scans separated by 10° rotations for a total of 360° around the breast. Except for very large breasts, data are obtained at 1.25-mm increments during translation.

There are advantages and disadvantages in using a high degree of compounding in the pulse echo images. Compound scanning (viewing of each point from multiple directions) is avoided in many modern ultrasound examinations to avoid loss of resolution due to refraction, transit time differences in various

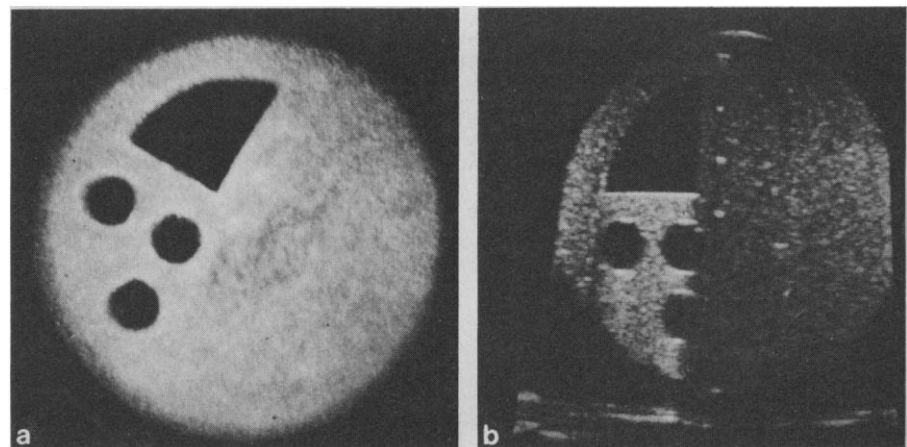


Fig. 1. Ultrasound images of a cylindrical breast phantom in water at 22°C. Small scatterers are distributed homogeneously in the fat-equivalent polymer. At 23°C ultrasound attenuation and speed of propagation are 1.1 dB/cm at 3 MHz and 1455 m/sec. Scatter-free regions are water. Four 0.5-mm-diameter nylon lines are echo-producing points to the right of the large anechoic wedge. (a) Compound image from prototype system obtained with linear scans every 10° over 360°. (b) Single-pass or single-view image obtained with a state-of-the-art commercial scanner.

tissues, instrument registration errors, and patient motion. However, motion is rarely a problem in this system, and compounding with enough views usually averages out most of the artifacts and provides much better delineation of breast architecture than does imaging with single views (5). Single-pass scanning for studying the textural details of masses and their attenuation and refractive properties is possible but is rarely necessary, given the information from the UCT images.

A simple illustration of the effect of extensive compounding is shown in Fig. 1. The overall structure of a large breast phantom is clearly revealed in the compound image (Fig. 1a) compared with the statistically noisy or speckled single-pass image (Fig. 1b). While some edges are sharper in the single-pass image, the homogeneous character of the main scat-

tering regions is represented with much greater fidelity in the compounded image.

Figure 2 shows examples of UCT and compounded pulse echo images in coronal planes and pulse echo images in transverse planes of the left breast of a 41-year-old woman. Pulse echo images (Fig. 2, a to c) are compared with the corresponding UCT images representing local attenuation coefficient (Fig. 2, e and f) and speed of sound (Fig. 2, h and i). A single sector image and a two-view compound image of a transverse plane in the same breast are also shown (Fig. 2, d and g). The latter images were obtained in transverse planes with a newly available commercial breast scanner (6).

A 1.8-cm-diameter tumor of poorly differentiated cells, diagnosed as infiltrating ductal carcinoma, was removed during mastectomy from the location of the visualized mass in this woman. In

Fig. 2, h and i, the carcinoma stands out strikingly as an isolated bright spherical mass of high speed of sound (1531 m/sec) in a predominantly fatty cross section of the breast with uniformly low speed of sound (1445 m/sec). In corresponding planes of the other breast, the highest speed of sound in any area greater than 1 cm² was 1455 m/sec. In the pulse echo images (Fig. 2, c, d, and g) the carcinoma is essentially echo-free; in the attenuation UCT images (Fig. 2, e and f) it appears to have attenuating borders. Although our diagnostic experience with the combination of all four of these images is limited, it is apparent that in this case the UCT speed-of-sound image served as a strong localizer of the carcinoma and helped to eliminate the possibility that the mass in the pulse echo images was a fatty infiltration. Fibroadenomas usually exhibit a higher echo level; and the central plane through a cyst would show reduced attenuation.

The most distinctive aspect of these images, however, is the detailed representation of the various breast structures provided by the compounded pulse echo images in the coronal planes. What appears as diffuse echoes throughout the large fatty areas just above or anterior to the mass in the transverse pulse echo scans (Fig. 2, d and g) is seen as a series of fatty nodules in the upper left and right of the coronal images (Fig. 2, a to c). Apparently this is due to the scan plane being normal to the fine connective tissue sheaths surrounding each small fatty nodule. Larger sheets of the connective tissue structure are apparent as longer lines of strong echoes in Fig. 2, a to c. The regions of uniformly high echogenicity probably are finely interspersed segments of glandular, fatty, and connective tissues in what remains of the mammary parenchyma.

Subsequent imaging of 15 patients and five mastectomy specimens with simultaneous pulse echo and through-transmission techniques has shown that detection and differential diagnosis of breast malignancy can still be difficult with smaller masses and in younger, denser breasts. As illustrated by a comparison of Fig. 3 with Fig. 2, the benign and malignant breast masses vary enough in their relation to various surrounding tissues to present apparently inconsistent appearances in ultrasound images. In Fig. 3a the infiltrating ductal carcinoma appears hyperechoic, although this most common breast malignancy generally is hypoechoic, as in Fig. 2.

Such apparent contradictions are not unique to diagnostic imaging with new techniques. As has been the case with

Fig. 2. Coronal and transverse pulse echo images and attenuation and speed-of-sound UCT images in a breast with infiltrating ductal carcinoma. In all the images the patient's left side is on the right. The patient's head is at the top in the seven coronal images. The plane in (a) is 8 cm posterior to the nipple; in (b), (e), and (h), 9 cm; and in (c), (f), and (i), 10 cm. Compounded pulse echo breast images obtained in the coronal planes of the UCT scanner are shown on the left (a to c). Single-sector and dual-sector images from a new commercial scanner are shown in (d) and (g), respectively, for a transverse plane approximately 14 mm inferior to the nipple. This early set of pulse echo images was obtained prior to the through-transmission scans, and the patient moved slightly between the pulse echo and UCT imaging. Figure 2c may correspond to (e) and (h).

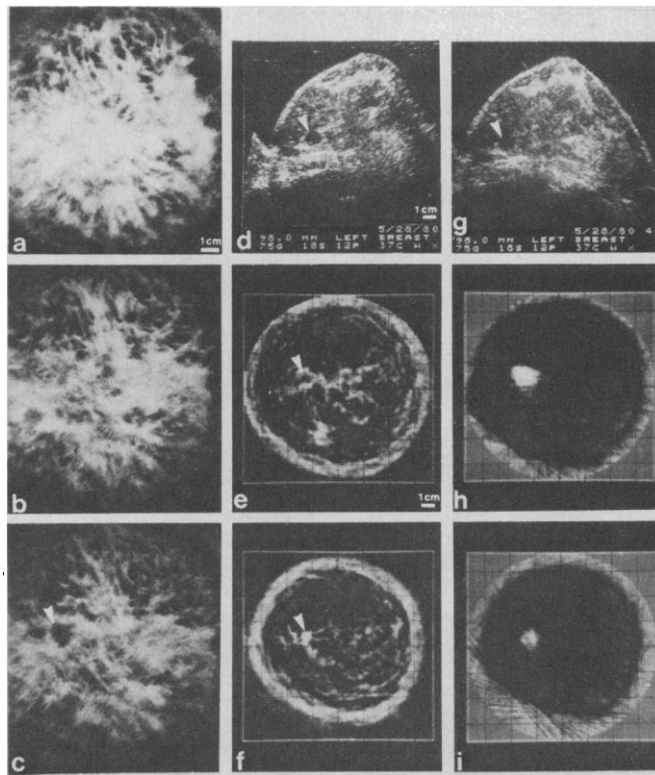
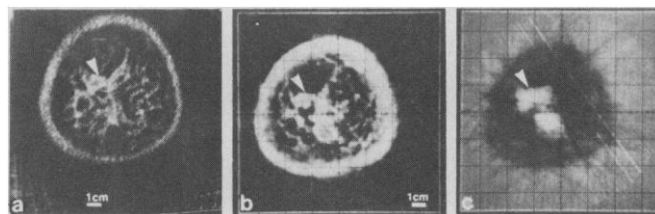


Fig. 3. (a) Pulse echo, (b) attenuation, and (c) speed-of-sound images obtained simultaneously in the right breast of a 55-year-old woman. The arrowheads indicate infiltrating ductal carcinoma (1510 m/sec). The lower bright spot represents the posterior portions of the subareolar tissues (1516 m/sec). The remainder of the breast plane is predominantly fatty tissue (1430 m/sec).



pulse echo ultrasound and, to an even greater extent, with x-ray mammography, extensive clinical experience and careful analytic studies correlating breast characteristics with image properties can lead to very useful diagnostic procedures. Many who have worked with pulse echo ultrasound consider it to be not only useful, but even the method of choice for diagnosing benign breast conditions and imaging young dense breasts (7). It probably is not far behind x-ray mammography in the general diagnosis of malignancy, but diagnostic accuracy of pulse echo imaging lags somewhat where relatively fatty breasts are concerned (8). As in the two examples shown here, however, the speed-of-sound images are most revealing in fatty breasts. It appears that the combination of UCT and pulse echo ultrasound is usually superior to either imaging technique alone.

We expect this diagnostic improvement to stimulate the development of clinical prototype pulse echo-UCT units capable of searching the breast for occult masses in a clinically acceptable examination time. Considerable improvement in image quality can be expected over the examples shown here. The signal-to-noise ratio in the pulse echo electronics of our system can be improved significantly, and progress is being made in the development of UCT attenuation and speed of sound techniques that will give higher resolution and a much more accurate quantitative representation of the bulk attenuation coefficient of the imaged tissues.

PAUL L. CARSON*
CHARLES R. MEYER*
ANN L. SCHERZINGER
THOMAS V. OUGHTON

Department of Radiology, Division of Radiological Sciences, School of Medicine, University of Colorado Health Sciences Center, Denver 80262

References and Notes

1. J. Greenleaf, S. Johnson, S. Lee, G. Herman, E. Wood, in *Acoustical Holography*, N. Booth, Ed. (Plenum, New York, 1974), pp. 591-603.
2. P. Carson, T. Oughton, W. Hendee, in *Ultrasound in Medicine*, D. H. White and R. W. Barnes, Eds. (Plenum, New York, 1976), pp. 391-400; J. Greenleaf, S. Johnson, W. Samayoa, F. Duck, in *Acoustical Holography*, N. Booth, Ed. (Plenum, New York, 1975), pp. 71-90; G. Glover and J. Sharp, *IEEE Trans. Sonics Ultrason.* **24**, 229 (1977); S. Johnson, J. Greenleaf, W. Samayoa, F. Duck, J. Sjostrand, *IEEE Ultrasound Symp. Proc.* (1975), pp. 46-51; P. Carson, T. Oughton, W. Hendee, A. Ahuja, *Med. Phys.* **4**, 302 (1977); J. Klepper, G. Brandenberger, L. Bussey, J. Miller, *IEEE Ultrasound Symp. Proc.* (1977), pp. 182-188; F. Duck and C. Hill, *Natl. Bur. Stand. (U.S.) Spec. Publ.* **525** (1979), pp. 247-251; A. Kak and K. Dines, *IEEE Trans. Biomed. Eng.* **25**, 321 (1978); R. Mueller, M. Kaveh, G. Wade, *Proc. IEEE* **67**, 567 (1979); E. Farrell, *Proc. IEEE Conf. Pattern Recog. Image Proc.* (1978), p. 8; S. Jones, F. Kitsen, P. Carson, E. Bayly, in *Frontiers of Engineering in Health Care* (Institute of Electrical and Electronics Engineers, New York, 1980), pp. 73-76; S. Norton and M. Linzer, *Ultrasound Imaging* **1**, 210 (1979).
3. G. Glover, *Ultrasound Med. Biol.* **3**, 117 (1977); J. Greenleaf, S. Johnson, R. Bahn, B. Rajogopalan, S. Keane, in *Computer-Aided Tomography and Ultrasonics in Medicine*, J. Raviv et al., Eds. (North-Holland, New York, 1979), pp. 125-136; P. Carson and A. Scherzinger, in *Clinics in Diagnostic Ultrasound: New Techniques and Instrumentation*, P. N. T. Wells and M. C. Ziskin, Eds. (Churchill Livingstone, New York, 1980), pp. 144-165.
4. P. Carson, A. Scherzinger, T. Oughton, J. Kubitschek, P. Lambert, G. Moore, M. Dunn, D. Dick, in *Application of Optical Instrumentation in Medicine: Proceedings*, W. R. Hendee and J. E. Gray, Eds. (Photo-Optical, Bellingham, Wash., 1979), vol. 35, p. 173 and pp. 372-381.
5. G. Kossoff, in *Clinics in Diagnostic Ultrasound: New Techniques and Instrumentation*, P. N. T. Wells and M. C. Ziskin, Eds. (Churchill Livingstone, New York, 1980), pp. 85-105.
6. D. Dick, R. Elliott, R. Metz, D. Rojohn, *Ultrasound Imaging* **1**, 368 (1979); A. Scherzinger, D. Dick, P. Carson, M. Johnson, J. Borgstede, *Proc. 24th Annu. Meet. Am. Inst. Ultrasound Med.* (1979), p. 108; W. Jobe, T. Stavros, D. Dick, *Proc. 25th Annu. Meet. Am. Inst. Ultrasound Med.* (1980), p. 66.
7. E. Kelly-Fry and P. Harper, *Proc. 24th Annu. Meet. Inst. Ultrasound Med.* (1979), p. 89; V. Maturio, N. Zusmer, A. Gilson, W. Smoak, W. Janowitz, J. Goddard, D. Dick, B. Bear, *Radiology* **137**, 457 (1980); T. Kobayashi, *Gray Scale Echography for Breast Cancer* (Hitachi Medical Corp., Tokyo, 1980), pp. 1-59; C. Cole-Beuglet, B. Goldberg, A. Kurtz, C. Rubin, S. Feig, G. Shaber, A. Patchefsky, *Proc. 25th Annu. Meet. Am. Inst. Ultrasound Med.* (1980), p. 60; S. Fields, *Ultrasound Imaging* **2**, 150 (1980).
8. J. Jellins, G. Kossoff, B. Barraclough, in *Recent Advances in Ultrasound Diagnosis*, A. Kurjak, Ed. (Excerpta Medica, Princeton, N.J., 1978), pp. 299-304.
9. Studies of patients and tissues were greatly aided by G. E. Moore, W. E. Jobe, S. G. Silverberg, M. L. Johnson, and R. E. Gerner. Physics and engineering support were provided by R. A. Belgam, T. L. Chenevert, D. E. Winans, W. R. Hendee, and D. E. Dick. This investigation was supported in part by National Cancer Institute grant R01 CA 25323 and National Science Foundation grant DAR: 7605944.

* Present address: Department of Radiology, Division of Radiological Physics and Engineering, School of Medicine, University of Michigan, Ann Arbor 48109.

18 May 1981; revised 13 August 1981

The Hagfish Slime Gland: A Model System for Studying the Biology of Mucus

Abstract. *The hagfish slime gland may provide a model system for studying certain aspects of the biology of mucus. Mucus is obtained in nonhydrated form by electrically stimulating the anesthetized hagfish and the secretions are stirred into ammonium sulfate. Centrifugation and filtration are then used to isolate the two major secretory products, mucous vesicles and threads. Specific advantages of the model and potential applications for research are discussed.*

The epidermally derived slime glands of the hagfish are primarily responsible for its capacity to produce copious quantities of mucus (1). In the Pacific hagfish *Eptatretus stouti* (2) there are approximately 150 of these glands (Fig. 1A) evenly spaced in two linear rows along its ventrolateral sides. Each slime gland is connected to the epidermal surface by a short duct, and the location of a gland is readily identified by its grossly visible pore on the epidermal surface (Fig. 1, A and C). The glands contain two large and morphologically distinct cell types: gland thread cells and gland mucous cells (Fig. 1B). The gland thread cell is filled with a long, coiled, proteinaceous thread (3); the gland mucous cell is filled with mucus-containing vesicles. The entire gland is surrounded by a connective tissue capsule, and outside the capsule are skeletal muscle fibers.

In this report we (i) propose that the hagfish slime gland may provide a model system for studying the biology of mucus, (ii) describe methods of secretory product acquisition, manipulation, and separation, (iii) point out some characteristics of the secretory products, and (iv) discuss possible research applications of the model.

Using a modification of an electrical

stimulation technique suggested by Ferry (4), we collected gram quantities of the two gland cell types and their products. Anesthetized hagfish (3) were draped over a beaker covered with absorbent paper and blotted dry. An electrical stimulator was used to administer a mild electric shock (5) to the skin adjacent to a slime gland pore (Fig. 1C). This caused the skeletal muscle cells outside the slime gland capsule to contract, expelling the contents of the gland onto the epidermal surface, where they formed a large white drop (Fig. 1, C and D). The glandular exudates were then harvested with a spatula (Fig. 1D) for processing.

One of many advantages to obtaining the glandular contents by this procedure is that hydration of the glandular exudates, which occurs during normal secretion, is circumvented. The extent to which these exudates are hydrated during normal secretion in an aqueous environment is indicated by stirring the electrically obtained exudates into seawater (Fig. 1, E to G) (6).

Although stirring the exudates into seawater provides useful information on mucus hydration, the extensive dilution and resultant high viscosity of the mucus makes biochemical characterization of the cellular components of the mucous